

# Noninvasive light-reflection technique for measuring soft-tissue stretch

John F. Federici, Nejat Guzelsu, Hee C. Lim, Glen Jannuzzi, Tom Findley, Hans R. Chaudhry, and Art B. Ritter

A novel, to our knowledge, sensor for measuring the stretch in soft tissues such as skin is described. The technique, which is a modification of two-dimensional polarization imaging, uses changes in the reflectivity of polarized light as a monitor of skin stretch. Measurements show that the reflectivity increases with stretch. Measurements were made on guinea pig skin and on nonbiological materials. The changes in reflectivity result from the changes that take place in the interface roughness between skin or material layers and the consequential changes in the diffuse reflective characteristics of the skin. Conceptually, as the roughness of an interface decreases, a smoother reflecting interface is produced, resulting in a commensurate increase in specular reflection. A simple roughness model correctly predicts the main experimental results. Results can be extended easily to real-time stretch analysis of large tissue areas that would be applicable for predicting stresses in skin during and after the surgical closure of wounds. © 1999 Optical Society of America

*OCIS codes:* 170.6930, 170.7050, 170.3890.

## 1. Introduction

The real-time measurement of the stretching of skin and the estimation of stresses in skin is an important problem in plastic surgery. Excessive tensile stresses delay wound healing and cause scar tissue and granulation.<sup>1-4</sup> Wounds created by accidents or surgical procedures involve trauma to both the skin and the underlying tissue. Wound healing proceeds through several stages, including an initial inflammatory response, cell proliferation, and cell migration. It has been well established that the cellular production and release of inflammatory mediators are altered by mechanical stress.<sup>5-7</sup> When the skin

is stretched during suturing stresses are produced. High tension across a sutured wound is likely to produce a stretched hypertrophic scar at that site.<sup>2</sup> Lesser scars are produced when the wound axis is placed parallel to the Langer (tension) lines compared with the case when the axis is across the lines.<sup>2,3</sup> Dehiscence, ischemia, or necrosis may be expected in regions of high stress through the compromise of circulation in the subdermal vascular plexus. Blood flow is inversely proportional to wound-closure tension, as has been observed in animal studies.<sup>8</sup> Therefore it is worthwhile to determine deformations and to predict stresses accurately for a given pattern of wound suturing. A preferred suturing pattern and wound geometry should produce low average tensile stresses with the lowest possible stress gradient at the critical points of the wound edges.<sup>9,10</sup>

In this paper an optically based technique for measuring skin stretch is reported. The optical properties of skin are related to its structure and its chemical composition.<sup>11</sup> Techniques of light reflection have been used to study the intrinsic properties of skin (such as the absorption and the scattering coefficients), and mathematical models have been developed to take these<sup>12-20</sup> into account. These studies were mainly used to determine the effects of pigments and hemoglobin on the reflection and the transmission characteristics of the skin that are due

---

J. F. Federici (federici@adm.njit.edu), H. C. Lim, and G. Jannuzzi are with the Department of Physics and H. R. Chaudhry is with the Department of Mathematics, New Jersey Institute of Technology, Newark, New Jersey 07102. H. R. Chaudhry is also with and T. Findley is with the Department of Physical Medicine and Rehabilitation and N. Guzelsu is with the Department of Osteopathic Sciences and Biomechanics, University of Medicine and Dentistry of New Jersey, School of Osteopathic Medicine, Stratford, New Jersey 08084. A. B. Ritter is with the Department of Physiology, University of Medicine and Dentistry of New Jersey, New Jersey Medical School, Newark, New Jersey 07103.

Received 13 August 1999; revised manuscript received 13 August 1999.

0003-6935/99/316653-08\$15.00/0

© 1999 Optical Society of America

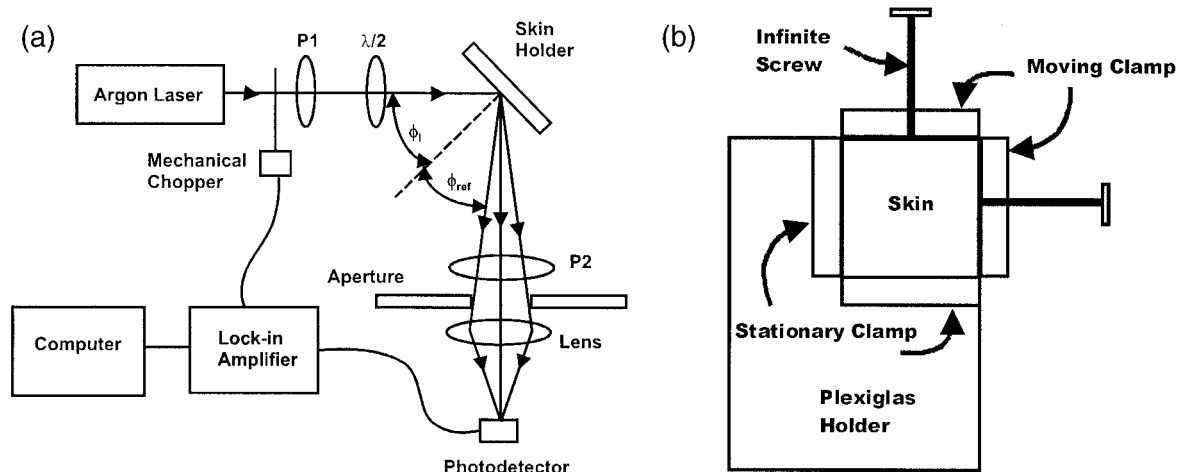


Fig. 1. (a) Experimental setup: Laser light is reflected from the middle portion of the skin sample where the stress should be uniform. P1 and P2 are polarizing filters for the incident and the reflected light, respectively. (b) Skin holder: Samples were clamped onto the Plexiglas holder by two stationary clamps and stretched through moving clamps. Moving clamps were pulled away from the Plexiglas holder by means of infinite screws.

to changes in the skin structure. Specific areas of study include skin erythema arising from UV light exposure and the mechanical compression of the skin.<sup>12-14,19-21</sup> Light scattering from collagen has been used to infer the orientation and the size of collagen fibers.<sup>22</sup>

When a beam of light reaches the skin surface, a small portion of it (5%) is reflected by the surface directly, whereas the rest is refracted and transmitted into the skin.<sup>11,12,23,24</sup> The direct reflection of light by a surface for which the angle of the reflected light is equal to the angle of the incident light (specular reflection) is related to the refractive-index change between the air and the reflecting medium.<sup>25</sup> By its nature the reflection of light from a turbid medium such as skin is diffuse rather than specular. The intensity and the angular distribution of diffuse reflection are determined by the transmission and the scattering properties of the skin tissue,<sup>12,19,20</sup> as well as by the polarization state of the incident light.<sup>26</sup> A portion of the light that is transmitted through the top layer of skin is scattered and absorbed by the underlying skin tissue. After multiple scattering events and reflections from the different layers of skin some of the transmitted light re-emerges through the air-stratum interface into the air as part of the total reflected light intensity.

The polarization properties of the reflected or the transmitted light depend on the number of scattering events that take place for each photon of light.<sup>27</sup> Photons that suffer virtually no scattering events (so-called ballistic photons) preserve their polarization properties. As photons suffer more and more scattering events, their final polarization state becomes more randomized. In the limit of many scattering events in a turbid tissue the outgoing photons (diffusive photons) are unpolarized and have equal-intensity components that are parallel and perpendicular to the polarization of the incident light.

In addition, the diffusive photons are not useful for tissue imaging because it is difficult to determine which areas of tissue were sampled by the diffusive photons. On the other hand, ballistic photons are partially reflected whenever there is a refractive-index difference on passage from one tissue layer into another. Hence the diffusive photons generally contribute to background noise that masks the tissue-imaging information carried by the ballistic photons. For linearly polarized incident light the reflected light, which contains the imaging information, maintains the same linear polarization. However, there is also a component of the diffusely reflected light that has the same polarization. In the two-dimensional (2-D) polarization-imaging technique subtracting the orthogonal component of the diffusely reflected light allows the background noise to be removed such that the skin tissue can be imaged.

In this study, we introduce a new, to our knowledge, technique based on a modification of the 2-D polarization-imaging method to measure skin stretch noninvasively by using the small changes that take place in the diffuse and the specular reflective properties of skin that are due to mechanical load.<sup>28</sup> The experimental setup, the preliminary data obtained from *in vitro* skin experiments, and the theoretical formulation of the technique are discussed.

## 2. Experimental Technique

### A. Optical Components

The experimental method is designed to measure small changes that take place in the reflection characteristics of the skin as a result of applied stretch (see Fig. 1). Linearly polarized light from an argon laser ( $\lambda = 488 \text{ nm}$ ,  $P \leq 1 \text{ mW}$ ) is reflected from the surface of the skin. Shorter wavelengths of light (488 nm) are used because they do not penetrate as deeply into the skin. Hence the reflectivity of this

light should be more sensitive to changes in the interface roughness between the various layers of skin near the surface. The light intensity is kept low enough to ensure a linear detector response (i.e., the voltage is proportional to the laser power) and to prohibit damage to the tissue.

For preliminary studies the angle of incidence  $\phi_i$  was varied from roughly  $20^\circ$  to  $70^\circ$ . The data presented in this study are measured by use of  $\phi_i \cong 57^\circ$  (which roughly corresponds to the Brewster angle). The reflected light is collected with a lens ( $f = 35$  mm) after it passes through a second polarizer (analyzer). The angle of the collected, reflected light and the aperture size are adjusted to collect the light in the specularly reflected direction. The solid angle of collection is approximately  $2.5 \times 10^{-2}$  sr. The polarization of the incident light and the analyzer can be set in one of two perpendicular orientations: parallel or perpendicular to the plane of incidence. The incident polarization is adjusted by use of a rotating half-wave plate. This adjustment ensures equal intensities in either plane of polarization. The laser power is detected by the mechanical chopping of the incident laser light and the utilization of a lock-in amplifier with phase-sensitive detection. The reflected power in both the parallel and the perpendicular polarizations is measured as a function of the incident-light polarization and the skin stretch. It is observed that the change in light intensity between the two perpendicular-polarization measurements of the analyzer is related to the amount of stretch in the skin. This method demonstrates a new device that can noninvasively measure skin stretch by light reflection.<sup>28</sup>

## B. Methods and Materials

A simple device was built to apply stretch to skin pieces, as shown in Fig. 1(b). The four sides of rectangular skin samples are clamped onto a Plexiglas stretching device. Two adjacent clamps can move with respect to the Plexiglas plate by use of infinite screws. The skin is held on the Plexiglas piece by two adjacent plastic pieces that are orthogonal to each other. The plastic pieces are attached to the Plexiglas piece by thumb screws. The skin is placed on an  $8.9 \text{ cm} \times 8.9 \text{ cm}$  area. The middle part of the Plexiglas plate is covered with a dull (nonshining), black, thin plastic piece. This plastic piece eliminates any reflection from the Plexiglas surface.

Four guinea pig skin samples (Hartley Guinea pigs, 500 to 550 g) were obtained from an outside source (Buckshire Corporation, Perkasie, Pennsylvania). The samples were shaved and delivered in saline solutions on the same day that the animals were sacrificed. To obtain a repeatable data set, we used the guinea pig spine orientation as an anatomical landmark. Square samples are taken from the skin pieces of which one side of the rectangle is taken parallel to the spine. The skin pieces are placed such that the side of the rectangle parallel to the spine is always parallel to one side of the stretching device. The skin is stretched parallel to the spine

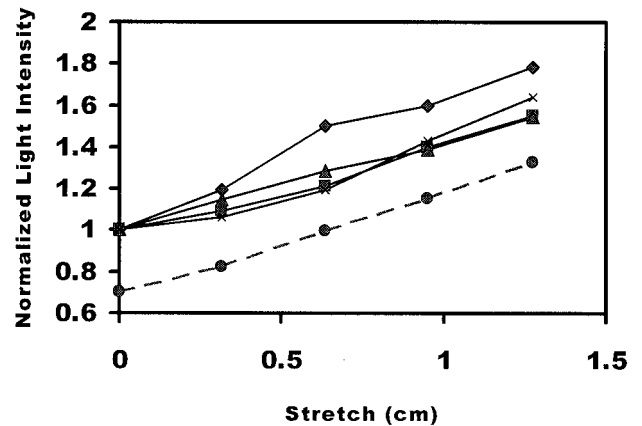


Fig. 2. Normalized reflectivity (reflected light intensity polarized parallel to the incident-light polarization minus the reflected light intensity polarized perpendicular to the incident-light polarization) plotted as a function of the stretch of skin taken parallel to the spine of the guinea pig. The reflectivity increases almost linearly with the applied stretch parallel to the spine. The four curves represent four skin samples. The dashed curve (offset for clarity) is the average of the four samples.

line and then released back to the original position. During the experiments the back side of the skin (the side facing the Plexiglas) is kept wet with a saline solution (pH of 7.4) to minimize friction between the two materials.

Owing to the preliminary nature of our simple skin-holder device, the stretch in one direction did not create a completely uniform deformation because the other sides of the skin parallel to the stretching direction were also clamped and could not follow the deformation uniformly. However, the central portion of the skin is subjected to a uniform deformation field that is parallel to the stretching direction. During the measurements laser light with a spot size of approximately 2 mm is reflected from this central portion of the skin. Various amounts of stretch, to as much as 1.5 cm (17%), are applied to the  $8.9 \text{ cm} \times 8.9 \text{ cm}$  samples. The infinite screw is turned between measurements by hand. After the maximum stretch is reached the skin sample is released to return to its original position with the same protocol. Some viscoelastic deformation takes place during the experiments. Usually the skin samples did not recover their original positions because of the viscoelastic deformations and also because of the friction between the Plexiglas surface and the skin, although this surface was kept wet with saline solution.

## 3. Results

Experiments on four skin samples from four different animals with a laser wavelength of 488 nm show that, when stretch is applied to samples of guinea pig skin samples taken parallel to the spine, a nearly linear relation between the amount of stretch and the reflected light intensity is measured (Fig. 2). In Fig. 2 the incident light is shown polarized perpendicularly to the plane of incidence and the spine direction.

As with the standard 2-D polarization technique, we compute the net reflected light intensity by taking the difference between the two perpendicular components of the reflected light (the component parallel to the polarization of the incident light minus the perpendicular component). The intensities are normalized with respect to the unstretched intensity. Similar results are obtained for incident light that is polarized parallel to the plane of incidence.

Because of viscoelastic deformations and residual friction between the skin and the Plexiglas, the skin samples did not recover their original reflectivity when returned to their original positions after stretching. Consequently, the absolute measured reflectivity for a particular stretch position would depend on prior stretching. However, the *slope* of the normalized reflectivity versus the stretch remained the same for all four samples. Repeated measurements on the same sample yields roughly the same slope with a slightly decreasing value with repeated stretches. This effect is probably due to material fatigue. The slopes of the normalized reflectivities, as determined by a least-squares fit, for the four samples shown in Fig. 2 are  $0.616 \pm 0.055$ ,  $0.441 \pm 0.031$ ,  $0.417 \pm 0.012$ , and  $0.517 \pm 0.064$ . The dashed curve of Fig. 2 is the average of the data points for the four samples and has a slope of  $0.498 \pm 0.015$ . Clearly, the data are reproducible from sample to sample.

We propose in the discussion below that interface roughness is responsible for the change in reflectivity with stretching. If this were true one would expect that the increase in reflection with stretching to be a *general* property of soft, stretchable materials and not to be restricted to biological tissues such as skin. To test this hypothesis, we measured the change in reflectivity of two different plastics as a result of stretching. The results are shown in Figs. 3 and 4. In both cases a linear change in reflectivity with stretching is observed. However, for stretches longer than approximately 1 mm the slope of the reflectivity for the sample shown in Fig. 3(a) becomes much flatter. The straight lines in Fig. 3(a) are linear regression fits to the data for stretches of less than 1 mm and greater than 1 mm. Figure 3(b) shows the net reflected light intensity (i.e., the difference between the two perpendicular components of the reflected light) for the fitted regression lines. Figure 4 shows the result for a polyvinyl chloride glove. No saturation of the reflectivity is observed with this sample.

#### 4. Simple Model of Skin Roughness

The relation between interface roughness and scattering can be explained if the incident light is regarded as being scattered from the specular-reflection or the transmission direction as it propagates through a rough surface. If the interface were rough the local angle of incidence for an individual light ray would depend on the location at which that ray encountered the interface (Fig. 5). Clearly, the presence of the rough interface would give rise to reflected laser power that would not be in the

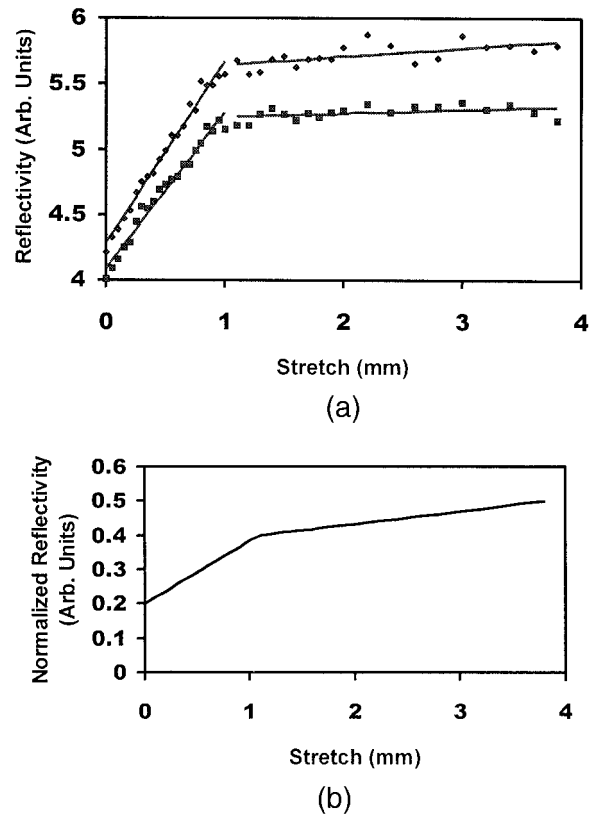


Fig. 3. (a) Reflectivity from a piece of stretched latex examination glove (unstretched length, 45 mm). The geometry of the stretch and the light polarization is the same as is shown for Fig. 2. Shown is the reflected light that is polarized parallel (filled diamonds) and perpendicular (filled squares) to the polarization of the incident light. The maximum change in reflectivity caused by stretching is approximately 35%. The maximum stretch is approximately 8.4%. The solid curves represent least-squares linear fits to the data for stretches of less than 1 mm (slopes of  $1.37 \pm 0.04$  and  $1.19 \pm 0.04$  for parallel and perpendicular polarization, respectively) and stretches of more than 1 mm (slopes of  $0.065 \pm 0.018$  and  $0.028 \pm 0.013$ , respectively). (b) Normalized reflectivity obtained by use of the least-squares fit results.

specular-reflection direction relative to the overall surface.

When the wavelength is short compared with the height and the spatial extent of the roughness (Mie scattering) the angular and the intensity dependences of the reflectivity are derived from the geometry of the interface, assuming that light is specularly reflected from each tilted element of the interface. This limit is appropriate for examining the reflection from skin. There are several mechanisms through which interface roughness affects the intensity of the reflected light:

- The direction of the reflected light from an interface depends on the local slope of the surface.
- The intensity of the light reflected or transmitted from an interface depends on the local angle of incidence and the polarization, which in turn depend on the local slope.

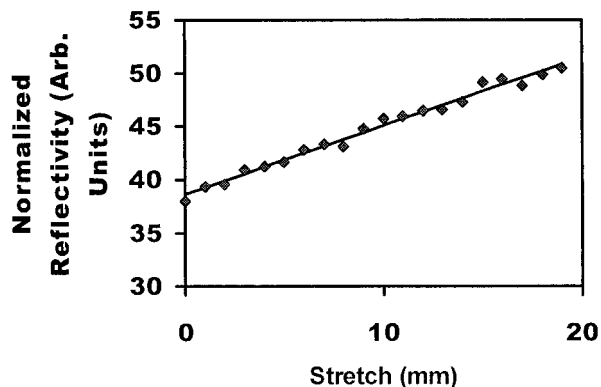


Fig. 4. Normalized reflectivity from a polyvinyl chloride examination glove (unstretched length of 45 mm). The geometry of the stretch and the light polarization are the same as were given for Fig. 2. The line is a fit to the data with a slope of  $0.644 \pm 0.018$ . No saturation in reflectivity is observed.

- Diffusely scattered light that is transmitted back from the skin to the air (the rightmost ray in Fig. 6) may pass through or be reflected from several rough interfaces. As with the transmission from air to skin, the intensity and the direction of the diffusely scattered light from skin to air depends on interface roughness.

In textbook treatments of tissue optics the reflectivity contribution derived from surface roughness

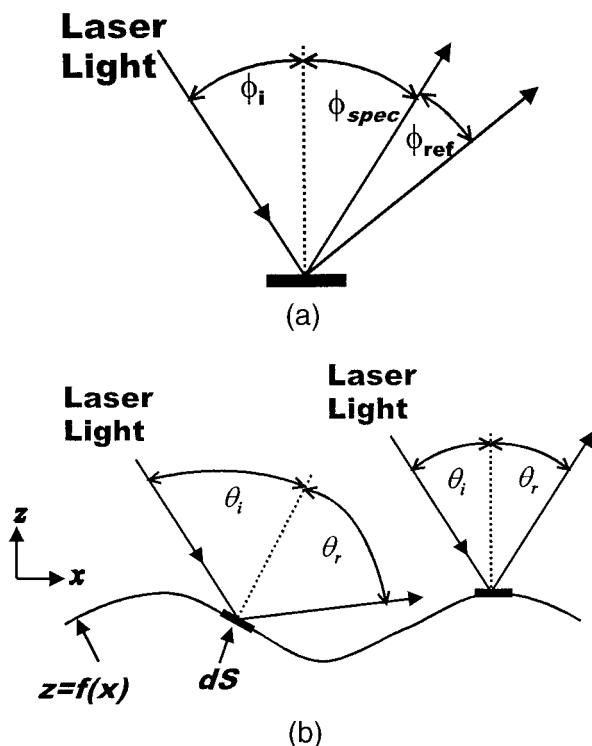


Fig. 5. (a) Flat surface: macroscopic definitions of the angles of incidence, specular reflection, and  $\phi_{ref}$  relative to the macroscopic orientation. (b) Rough surface: microscopic definitions of the angles of incidence and reflection for a rough interface.

usually is neglected or incorporated into an overall attenuation coefficient for scattering. Although neglecting the surface roughness is appropriate for the stratum corneum layer of skin (Fig. 6), underlying layers of skin such as the epidermis and the dermis are characterized by numerous rough interfaces such as the boundary between the epidermis and the dermis. The papillary layer beneath this epidermis-dermis junction consists of numerous highly sensitive and vascular eminences, termed papillae, that project perpendicularly. This region is closely related to rich capillary beds in the dermis. This capillary structure supplies nutrients to the epidermis. The roughness of this junction allows the tight binding between the epidermis and the dermis and also allows a large surface area for nutritional exchange.<sup>29</sup>

The experimental configuration is chosen to accentuate the contribution to the reflectivity from the outermost 100  $\mu\text{m}$  of skin. It is well known that shorter wavelengths of light (blue) do not penetrate as far into the skin as do longer wavelengths (red). Thus shorter wavelengths of light (488 nm) should be more sensitive to interface-roughness changes than red light would be. For *in vivo* samples the reflectivity of red light is also strongly influenced by the presence of blood in the underlying tissue.

To demonstrate the effect of large-scale roughness on the reflectivity from soft tissue, we start with a simple 2-D model for the roughness  $z$  of an interface<sup>30</sup>:

$$z = A \sin(gx), \quad (1)$$

where  $A$  is the height of the roughness with a wavelength of  $2\pi/g$ . This periodic model was suggested originally for the surface roughness of skin and is used to explain how the surface patterns of the skin change as a result of tension loads.<sup>30</sup> Clearly, the assumptions made in this model and the subsequent derivation are an oversimplification of the problem. However, this simple model demonstrates that interface roughness, which decreases with increasing stretch, could explain three of our experimental results: (a) the observed increase in the diffusely reflected light intensity, (b) the observed increase in the specularly reflected light intensity, and (c) the linear relation between tissue stretch and reflectivity.

Although the periodic-roughness assumption is not strictly true, the physiology of the various skin layers<sup>29</sup> and topological measurements of skin<sup>31</sup> show quasi-periodic interfaces between different layers of skin. Therefore a periodic-roughness rather than a random-roughness model appears to be appropriate, with the spatial scale of the periodic roughness representing a characteristic roughness scale of the skin.

As a further simplification, interference among the various rays of light reflecting from the surface (laser speckle) can be ignored. This approximation is valid because of the long integration time for data acquisition by use of phase-sensitive detection (a 1-s time constant) and the fairly large solid angle of detection. The 1-s integration time is much longer than the

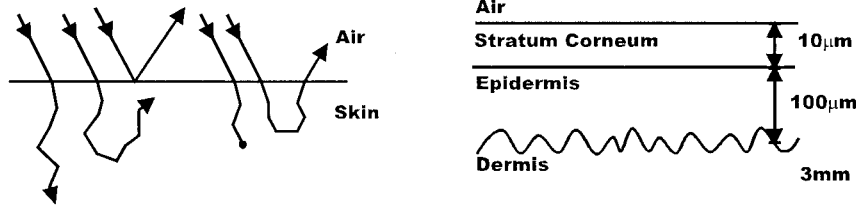


Fig. 6. Schematic diagrams of the optical pathways and the structure of the skin.

correlation time of laser-induced speckles so that temporally the speckle effect is averaged out.<sup>26</sup> In addition, reflected light is collected over a fairly large solid angle. Because all the collected light is detected by a single-element photodiode, any spatial fluctuations in light intensity caused by laser speckle are averaged out.

For the theoretical analysis reflected light from the skin is collected with a lens that is oriented at an angle  $\phi_{\text{ref}}$  and that collects light within an angle of  $\Delta\phi_{\text{ref}}$  (Fig. 5). The collected light is focused onto a single-element detector. An angle of  $\phi_{\text{ref}} = 0$  corresponds to the specular-reflection direction. The incident light is assumed to be of uniform intensity  $I_0$  and to illuminate an area of dimensions  $L_x \times L_y$  of the surface. The total power detected is

$$P(\phi_i) = - \int_S \int_{\text{angles}} I_0 \hat{k} \cdot d\mathbf{S} r(\theta_i) \delta(\theta_i = \phi_i + \phi_{\text{ref}}/2) d\phi_{\text{ref}}. \quad (2)$$

The integration is over the entire solid angle of the reflected light that is captured by the focusing lens and over the surface  $S$  of the reflecting tissue. The  $\delta$  function selects out surfaces that are in the range of correct tilts such that the reflected light is within the acceptance angle  $\Delta\phi_{\text{ref}}$ ;  $r(\theta_i)$  is the Fresnel reflection (power) coefficient,  $\hat{k}$  is a unit vector pointing in the direction of the incident light ray, and  $d\mathbf{S}$  is the element of surface area whose vector point is normal to the surface, as shown in Fig. 5.

For a given surface profile of  $z = A \sin(gx)$ , the normal to the surface is given by

$$\hat{n} = \frac{\nabla[z - \sin(gx)]}{|\nabla[z - \sin(gx)]|} = \frac{[\hat{z} - \hat{x}Ag \cos(gx)]}{\{1 + [Ag \cos(gx)]^2\}^{1/2}}. \quad (3)$$

For a surface element to reflect light into the detection angle  $\phi_{\text{ref}}$  its normal vector must be

$$\hat{n} = \hat{z} \cos(\phi_{\text{ref}}/2) + \hat{x} \sin(\phi_{\text{ref}}/2). \quad (4)$$

Equating Eqs. (3) and (4) shows that, when  $x$  satisfies

$$\tan(\phi_{\text{ref}}/2) = -Ag \cos(gx), \quad (5)$$

light rays will be reflected into the detector. The vector properties of the surface integral can be written as

$$\hat{k} \cdot d\mathbf{S} = \hat{k} \cdot \hat{n} dS, \quad (6)$$

where  $dS = dx dy |\nabla[z - \sin(gx)]|$  and the ranges of  $dx$  and  $dy$  are determined from solutions for  $x$  of Eq. (5), where  $\phi_{\text{ref}}$  varies between  $\phi_{\text{ref}} \pm \Delta\phi_{\text{ref}}$ .

As a simple example, consider light detected in the specular direction ( $\phi_{\text{ref}} = 0$ ) within a collection angle of  $\pm\Delta\phi_{\text{ref}}$ . Using Eqs. (5) and (6) shows that the total power detected is

$$P(\phi_i) = - \iint dx dy I_0 \hat{k} \cdot \nabla[z - A \sin(gx)] \times r(\theta_i = \phi_i + \phi_{\text{ref}}/2), \quad (7)$$

where

$$\hat{k} = -\hat{z} \cos \phi_i + \hat{x} \sin \phi_i \quad (8)$$

and the range of  $x$  is given by the solution of Eq. (5) when  $-\Delta\phi_{\text{ref}} < \phi_{\text{ref}} < \Delta\phi_{\text{ref}}$ . Because the integral is independent of the variable  $y$ , the integral over  $y$  yields just  $L_y$ , the length along the  $y$  axis. For small stretching and a small collection angle, one can consider  $r(\theta_i)$  to be approximately constant with the ranges of  $dx$  and  $dy$  that contribute to the integral's changing with stretch. Furthermore, the fact that the topology of the surface is periodic can be exploited. Each cycle of the fluctuation of the wavelength  $2\pi/g$  produces two areas that will reflect into the detector. If the integration over  $dx$  were restricted to one wavelength of roughness the integral should be multiplied by  $2L_x g / 2\pi \equiv N$ , which represents the number of reflecting areas. The total power detected is then approximately

$$P(\phi_i) = NI_0 L_y r(\phi_i) \int dx [\cos \phi_i + Ag \sin \phi_i \cos(gx)]. \quad (9)$$

The limits of integration are determined by Eq. (5). For low values of  $\Delta\phi_{\text{ref}}$  the ranges of  $dx$  that contribute to the integral are  $\pi/(2g) \pm \Delta x$  and  $3\pi/(2g) \pm \Delta x$ . In the limit of a flat surface,  $Ag = 0$ , and the limits of integration are between 0 and  $\pi/g$ . In this flat-surface limit the power detected is

$$\begin{aligned} P(\phi_i) &= NI_0 \pi L_y r(\phi_i) \cos \phi_i / g_i \\ &= I_0 L_x L_y r(\phi_i) \cos \phi_i \\ &= P_0 r(\phi_i), \end{aligned} \quad (10)$$

which is just the reflectivity of a flat surface.

Two regimes of roughness can be considered:  $Ag \gg 1$  (very rough surfaces) and  $Ag \ll 1$  (slightly

rough surfaces). In the very-rough-surface limit ( $Ag \gg 1$ ) only a small fraction of the interface surface contributes to the detected reflected light. In this limit the integral is approximately

$$P(\phi_i) = NI_0 L_y r(\phi_i) 2 \cos \phi_i \Delta x, \quad (11)$$

where  $\Delta x$  represents the linear extent of the surface that contributes to the reflectivity. Using  $\Delta\phi_{\text{ref}}/2 = Ag^2 \Delta x$  as an approximate form of Eq. (5) for a small cone of detected angles allows the detected power to be written as

$$P(\phi_i) = P_0 r(\phi_i) \frac{\Delta\phi_{\text{ref}}}{\pi Ag}. \quad (12)$$

For our experimental configuration  $P_0$ ,  $\phi_i$ , and  $\Delta\phi_{\text{ref}}$  are kept constant. As the soft tissue is stretched, both the amplitude  $A$  and the wave number  $g$  decrease, leading to an *increase* in the detected power. As the interface roughness *decreases*, the detected power in the specular direction *increases*. This increase in detected power is observed with our soft-tissue sensor.

Using a simplified model for the mechanical properties of the skin allows the change in reflectivity for small stretches to be determined. As an interface within the skin (e.g., the epidermis–dermis interface) and other biological elements in the skin are stretched, the surface, the interface, and the extracellular matrix flatten out subject to the constraint that the length of the surface remain constant. Using the profile of the surface of  $z = A \sin(gx)$  leads to the length of the surface being calculated as

$$\begin{aligned} L &= \int \{|\nabla[z - A \sin(gx)]|\}^{1/2} dx \\ &= M \int_0^{2\pi/g} \{[1 + A^2 g^2 \cos^2(gx)]\}^{1/2} dx, \end{aligned} \quad (13)$$

where  $M$  is the number of oscillations of the surface and the integral is over one oscillation of the surface. As the skin is stretched, the height of the interface roughness  $A$  and the scale length  $2\pi/g$  change in such a way that the length of the surface remains constant. For  $Ag \gg 1$  the integral becomes

$$L \cong M \int_0^{2\pi/g} Ag |\cos(gx)| dx = 4MAg. \quad (14)$$

Let the wavelength of one oscillation be  $s = 2\pi/g$  so that the path length of the surface becomes

$$L = M8\pi A/s, \quad Ag \gg 1. \quad (15)$$

As the tissue is stretched,  $A$  and  $s$  change such that  $L$  remains constant. Substituting this result into the expression for reflected power [Eq. (12)] yields

$$P(\phi_i) = I_0 L_y r(\phi_i) \frac{\Delta\phi_{\text{ref}}}{\pi} \frac{s}{2\pi} \cos \phi_i \frac{4M}{L}, \quad Ag \gg 1. \quad (16)$$

It is interesting to note that, in the limit of high roughness ( $Ag \gg 1$ ), the theoretical result shows that the reflected power is linearly proportional to the stretch  $s$ , in agreement with the experimental results. Typically, for skin, the roughness of the epidermis–dermis interface is greater than the skin–air roughness,<sup>29,30</sup> and the roughness of the epidermis–dermis interface satisfies the  $Ag \gg 1$  high-roughness condition.<sup>29</sup> Our experimental and theoretical results suggest that the changing roughness of the epidermis–dermis interface may be primarily responsible for the observed changes in light reflection owing to skin stretch.

As shown in Figs. 3 and 4, the change in reflectivity with stretching is a general property of materials and is not limited to biological tissues. The saturation of the reflectivity with stretching for the latex material shown in Fig. 3 can be explained with the interface-roughness model. As a material stretches, there clearly must be a point of saturation: After the roughness of the surface is removed by means of stretching (i.e., the surface is as smooth and as mirrorlike as possible) additional stretching will not increase the reflectivity.

## 5. Discussion

Our method uses changes in the diffuse-reflectance properties of skin that are due to mechanical deformation to determine soft-tissue deformations noninvasively. A small spot size (gauge length) with a miniaturized detector and a fiber-optic delivery–detection system would allow surgeons to determine the stretch of soft tissues in real time. One could improve the utility of the technique by imaging stretch patterns from a large area of tissue. Our technique can easily be extended to an imaging technology by the replacement of the single-element photodetector with a CCD camera. The geometry of the imaging optics is similar to the 2-D polarization-imaging technique.<sup>27</sup> Experiments that image a nonuniform stretch pattern by use of our technique are underway and are intended for another report.

Measuring the tension in wound closures,<sup>32</sup> skin flaps,<sup>33</sup> and tissue expanders<sup>34</sup> will help surgeons to treat wound closure and healing in patients more successfully by minimization of scar tissue and maximization of the speed of treatment, especially after accidents and burns, from knowledge of how much the skin can be stretched at each treatment step. The information will be very useful, in particular, in plastic surgery because the effects of tension forces on the successful outcome of surgery are crucial. The measurement technique can be used to determine the excess mechanical deformations of internal vessel walls or internal organs around a surgical site. This information could be useful in avoiding injury to the surrounding tissue, as the optimum amount of force could be applied during suturing. By use of a CCD imaging technique the stretch sensor could give instant information on the stress concentration of tissues that is due to different surgical procedures.

Further applications could be found in mechanical

experiments to determine the deformation of the diffuse-reflectance materials as a noncontact extensometer. With a very small spot size (gauge length) the technique could be superior to the existing technology of video extensometers. Determining the mechanical properties of soft tissues and also obtaining the mechanical properties of soft artificial biomaterials will advance the fields of biomechanics and biomaterials in which real-time, *in situ* imaging measurements of such properties are critical.

Helpful discussions with J. M. Joseph are acknowledged.

## References

1. C. Cacou, J. M. Anderson, and I. F. K. Muir, "Measurement of closing force of surgical wounds and relation to the appearances of resultant scars," *Med. Biolog. Eng. Comput.* **32**, 638–642 (1994).
2. T. Gibson, "Physical properties of skin," in *Plastic Surgery Volume 1: General Principles*, J. G. McCarthy, ed. (Saunders, Philadelphia, Pa., 1990), pp. 207–220.
3. C. Cacou and I. F. K. Muir, "Effects of plane mechanical forces in wound healing in humans," *J. R. Coll. Surg. Edinburgh* **40**, 38–41 (1995).
4. B. D. Bucalo and M. Iriondo, "Photoelastic models of wound closure stress," *Dermatol. Surg.* **21**, 210–212 (1995).
5. B. Sumpio, A. Baner, and L. Levin, "Mechanical stress stimulates aortic endothelial cells to proliferate," *J. Vasc. Surg.* **6**, 252–256 (1987).
6. B. Sumpio and M. Windmann, "Enhanced production of an endothelium derived contracting factor by endothelial cells subject to pulsative stretch," *Surgery* **108**, 277–282 (1990).
7. M. U. Nollert, E. R. Hall, S. G. Eskin, and L. V. McIntire, "Effect of flow on arachidonic acid metabolism in human endothelial cells," *Biochim. Biophys. Acta* **1005**, 72–78 (1989).
8. W. F. Larabee, G. A. Holloway, and D. Sutton, "Wound tension and blood flow in skin flaps," *Ann. Otol. Rhinol. Laryngol.* **93**, 112–115 (1984).
9. H. R. Chaudhry, B. Bukiet, M. Siegel, T. Findley, A. B. Ritter, and N. Guzelsu, "Optimal patterns for suturing wounds," *J. Biomech.* **31**, 653–662 (1998).
10. H. R. Chaudhry, B. Bukeit, T. Findley, and A. B. Ritter, "Evaluation of residual stress in rabbit skin and the relevant material constants," *J. Theor. Biol.* **192**, 191–195 (1998).
11. R. R. Anderson and J. A. Parrish, "Optical properties of human skin," in *The Science of Photomedicine*, J. D. Regan and J. A. Parrish, eds. (Plenum, New York, 1982), pp. 147–194.
12. J. B. Dawson, D. J. Barker, D. J. Ellis, E. Grassam, J. A. Cotterill, G. W. Fisher, and J. W. Feather, "A theoretical and experimental study of light absorption and scattering by *in vivo* skin," *Phys. Med. Biol.* **25**, 695–709 (1980).
13. P. H. Andersen and P. Bjerring, "Spectral reflectance of human skin *in vivo*," *Photodermatol. Photoimmunol. Photomed.* **7**, 5–12 (1990).
14. P. H. Andersen and P. Bjerring, "Noninvasive computerized analysis of skin chromophores *in vivo* by reflectance spectroscopy," *Photodermatol. Photoimmunol. Photomed.* **7**, 249–257 (1990).
15. M. J. C. Van Gemert, S. L. Jacques, H. J. C. M. Sterenborg, and W. M. Star, "Skin optics," *IEEE Trans. Biomed. Eng.* **36**, 1146–1154 (1989).
16. W. F. Cheong, S. A. Prahl, and A. J. Welch, "A review of the optical properties of biological tissues," *IEEE J. Quantum Electron.* **26**, 2166–2185 (1990).
17. B. C. Wilson and S. L. Jacques, "Optical reflectance and transmittance of tissues: principles and applications," *IEEE J. Quantum Electron.* **26**, 2186–2199 (1990).
18. S. L. Jacques, "The role of skin optics diagnostic and therapeutic uses of lasers," in *Lasers in Dermatology*, R. Steiner, R. Kaufmann, M. Landthaler, and O. Braun-Falco, eds. (Springer-Verlag, Berlin, 1991), pp. 1–21.
19. H. Zeng, C. MacAulay, B. Palcic, and D. I. McLean, "A computerized autofluorescence and diffuse reflectance spectroanalyser system for *in vivo* skin studies," *Phys. Med. Biol.* **38**, 231–240 (1993).
20. Y. P. Sinichkin, S. P. Uts, and E. A. Pilipenko, "Spectroscopy of human skin *in vivo*: 1. Reflection spectra," *Phys. Opt.* **80**, 228–234 (1996).
21. P. Bjerring and P. H. Andersen, "Skin reflectance," *Spectrophotom. Photodermatol. Photoimmunol. Photomed.* **4**, 167–171 (1987).
22. A. G. Ferdman and I. V. Yannas, "Scattering of light from histologic sections: a new method for the analysis of connective tissue," *J. Invest. Dermatol.* **100**, 710–716 (1993).
23. R. R. Anderson and J. A. Parrish, "The optics of human skin," *J. Invest. Dermatol.* **77**, 13–19 (1981).
24. V. V. Tuchin, "Lasers and fiber optics in biomedicine," *Laser Phys.* **3**, 767–820 (1993).
25. E. Hecht, *Optics*, 3rd ed. (Addison Wesley, Reading, Mass., 1997).
26. B. D. Cameron, M. J. Rakovic, M. Mehrubeoglu, G. Kattawar, S. Rastegar, L. V. Wang, and G. L. Cote, "Measurement and calculation of the two-dimensional backscattering Mueller matrix of a turbid medium," *Opt. Lett.* **23**, 485–487 (1998).
27. S. G. Demos and R. R. Alfano, "Optical polarization imaging," *Appl. Opt.* **36**, 150–155 (1997).
28. N. Guzelsu, T. W. Findley, J. F. Federici, H. R. Chaudhry, and A. B. Ritter, "Apparatus and method for noninvasive measurement of stretch," U.S. patent pending, application 27 October 1998.
29. P. L. Williams and R. Warwick, eds., *Gray's Anatomy*, 36th ed. (Saunders, Philadelphia, Pa., 1980), pp. 1216–1226.
30. J. Ferguson and J. C. Barbenel, "Skin surface patterns and the directional mechanical properties of the dermis," in *Bioengineering and the Skin*, R. Marks and P. A. Payne, eds. (MTP, Lancaster, Pa., 1981), pp. 83–92.
31. M. Assoul, M. Zahidi, P. Corcuff, and J. Mignot, "Three-dimensional measurements of skin surface topography by triangulation with a new laser profilometer," *J. Med. Eng. Technol.* **18**, 11–21 (1994).
32. E. E. Peacock, Jr., and I. K. Cohen, "Wound healing," in *Plastic Surgery Volume 1: General Principles*, J. G. McCarthy, ed. (Saunders, Philadelphia, Pa., 1990), pp. 161–181.
33. R. K. Daniel and C. L. Kerrigan, "Principles and physiology of skin flap surgery," in *Plastic Surgery Volume 1: General Principles*, J. G. McCarthy, ed. (Saunders, Philadelphia, Pa., 1990), pp. 275–328.
34. L. C. Argenta and E. D. Austad, "Principles and techniques of tissue expansion," in *Plastic Surgery Volume 1: General Principles*, J. G. McCarthy, ed. (Saunders, Philadelphia, Pa., 1990), pp. 475–507.